

4 Rare Kaon Decays at the Brookhaven AGS

H. Kaspar (visiting scientist), P. Robmann, A. van der Schaaf, S. Scheu,
A. Sher (until January 2004) and P. Truöl

Our research program at the Brookhaven National Laboratory's Alternating Gradient Synchrotron (AGS) focuses on rare kaon decays. Only at the AGS intense low-momentum neutral and charged kaon beams are still available today. Though Experiment BNL E-865 finished data-taking in 1998 the analysis of its high statistics data sample on semi-leptonic and leptonic charged kaon decays still supplies novel results. The KOPIO-experiment has been approved for funding by the U.S. National Science Foundation, and its planning concentrates now on the construction of the various detector subsystems and development of a suitable pulsed neutral kaon beam.

4.1 BNL E-865: first observation of the decay $K^+ \rightarrow e^+ \nu_e \mu^+ \mu^-$

in collaboration with:

Paul-Scherrer-Institut, CH-5234 Villigen; Brookhaven National Laboratory, Upton, NY-11973, USA; University of New Mexico, Albuquerque, NM-87131, USA; University of Pittsburgh, Pittsburgh, PA-15260, USA; Yale University, New Haven, CT-06511, USA; Institute for Nuclear Research, Academy of Sciences 117 312 Moscow, Russia

The radiative kaon and pion decays and their internally converted partners

$$K_{\ell 2\gamma} : K^+ \rightarrow \ell^+ \nu_\ell \gamma, \quad K^+ \rightarrow \ell^+ \nu_\ell \ell'^+ \ell'^-, \quad \ell(\ell') = e, \mu$$

$$\pi_{e 2\gamma} : \pi^+ \rightarrow e^+ \nu_e \gamma, \quad \pi^+ \rightarrow e^+ \nu_e e^+ e^-$$

are both an important source of input information as well as a test of the successful chiral perturbation theory (ChPT) (1), the low energy version of quantum chromodynamics. The pion decays were studied during the late eighties in pioneering experiments by the SINDRUM- (2) and the Lausanne-Zürich-collaborations (3) at PSI. In both these collaborations teams from our institute played a prominent role. Radiative pion decay is presently being re-investigated (see Sec. 6.1). Figure 4.1 indicates which processes are to be considered in the construction of the decay amplitudes. The inner bremsstrahlung part, where the virtual photon is radiated either by the decaying meson or by the final state lepton can be calculated in a straightforward and parameter free manner. More interesting is the structure dependent part, which is characterized by the axial vector and vector form factors F_A and F_V and the form factor R , which are the quantities of interest. For example, F_A of the pion fixes one of the terms in

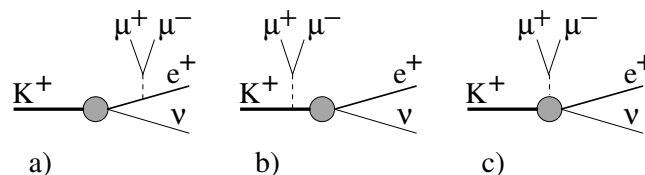


Figure 4.1:

Inner bremsstrahlung (a,b) and structure dependent (c) contributions to the radiative kaon decay $K^+ \rightarrow e^+ \nu_e \mu^+ \mu^-$.

the ChPT-Hamiltonian.

From our experiment E865 (4) we already published results on the radiative decays $K^+ \rightarrow \mu^+ \nu_\mu e^+ e^-$ and $K^+ \rightarrow e^+ \nu_e e^+ e^-$ (5). We have now been able to observe for the first time the decay $K^+ \rightarrow e^+ \nu_e \mu^+ \mu^-$ (6), and determined its branching ratio to

$$B(K^+ \rightarrow e^+ \nu_e \mu^+ \mu^-) = (1.72 \pm 0.37 (\text{stat.}) \pm 0.17 (\text{syst.}) \pm 0.19 (\text{mod.})) \times 10^{-8}$$

In this decay the inner bremsstrahlung contribution is electron helicity suppressed and negligible compared to the structure dependent part, a situation quite different from that in radiative pion decay. ChPT relates F_A and F_V for kaon and pion, and R to the kaon and pion charge radii. Starting from our sample of close to 450'000 triggered $K^+ \rightarrow \pi^+ \pi^- e^+ \nu_e$

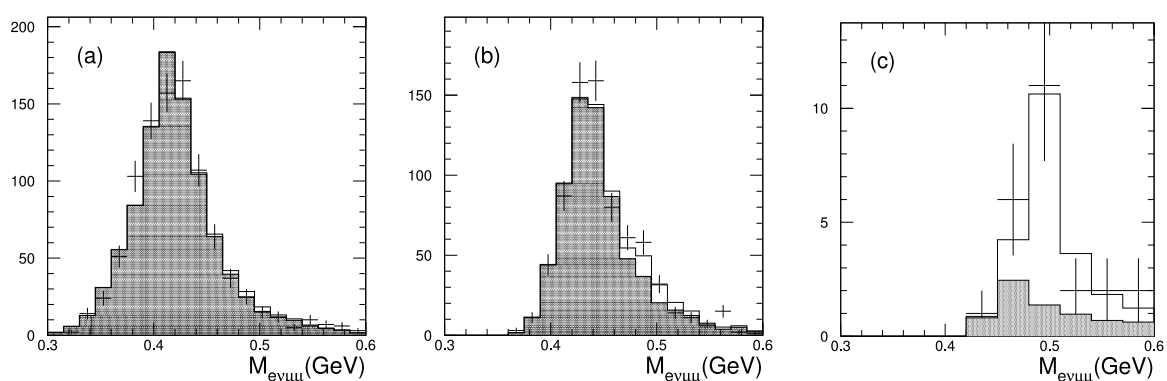


Figure 4.2:

$M_{e\nu\mu\mu}$ invariant mass distribution for events surviving all selection criteria for three bins of the invariant mass $M_{e\mu\mu}$: a) 282.5 to 355 MeV; b) 355 to 427.5 MeV; c) above 427.5. The crosses are the measured data, the histogram is the fitted spectrum consisting of background (shaded) and signal contributions.

(K_{e4}) events (7) 1834 events survived the muon identification cuts, which require a signal in the electromagnetic calorimeter consistent with a minimum ionizing particle and a range in the muon identifier consistent with the measured momentum. This sample is however still dominated by background from K_{e4} or K_τ ($K^+ \rightarrow \pi^+ \pi^- \pi^+$) decays with misidentified pions and from accidental overlays of two decays with the correct particles in the final state. As is shown in Fig. 4.2 these events are characterized by a lower reconstructed $e\mu\mu$ -invariant mass than expected for signal events, their kinematical properties being well understood and represented by the Monte Carlo simulation. The probability that a statistical fluctuation of the background leads to the observed signal of about 17 events with the expected $e\mu\mu\nu$ invariant mass near M_K is less than 10^{-6} . The branching ratio was determined normalizing to K_{e4} decay (7). The systematic error arises predominantly from the uncertainty of the muon identification, while the model dependence accounts for the extrapolation to areas of the phase space not accessible in our experiment. The form factors were fixed at the values determined by us in the other radiative kaon decay channels (5). The measured branching ratio is slightly larger than the ChPT-prediction (8) of 1.12×10^{-8} .

- [1] S. Weinberg, *Physica* **96A**, 327 (1979); J. Gasser and H. Leutwyler, *Ann. Phys.* **158**, 142 (1984); *Nucl. Phys.* **B250**, 465 (1985); for a recent review see *Effective field theories of QCD*, Proc. 264th WE-Heraeus-Seminar, Bad Honnef, Germany (2001), J. Bijnens, U.G. Meißner, and A. Wirzba eds., hep-ph/201266, and references therein.
- [2] S. Egli *et al.* (SINDRUM-coll.), *Phys. Lett.* **B222** (1989), 533; *ibid.* **B175** (1986), 97.
- [3] A. Bay *et al.* (Lausanne-Zürich-coll.), *Phys. Lett.* **B174** (1986), 445.

- [4] **A Large Acceptance, High Resolution Detector for Rare K^+ -decay Experiments**, R. Appel *et al.* (E865-coll.), Nucl. Instr. Methods Phys. Res. **A479**, 349 (2002).
- [5] **Experimental Study of the Radiative Decays $K^+ \rightarrow \mu^+ \nu_\mu e^+ e^-$ and $K^+ \rightarrow e^+ \nu_e e^+ e^-$** , A.A. Poblaguev *et al.* (E865-coll.), Phys. Rev. Lett. **89** (2002), 061803-1.
- [6] **First Observation of the Decay $K^+ \rightarrow e^+ \nu_e \mu^+ \mu^-$** , H. Ma *et al.*, *subm. to Phys. Rev. D*.
- [7] **High Statistics Measurement of K_{e4} Decay Properties**, S. Pislak *et al.* (E865-coll.), Phys. Rev. **D67**, 072004-1 (2003); Phys. Rev. Lett. **87**, 221801-1 (2001).
- [8] J.Bijnens, G. Ecker, and J. Gasser, Nucl. Phys. **B396**, 81 (1993).

4.2 KOPIO: a study of the CP-violating rare decay $K_L^0 \rightarrow \pi^0 \nu \bar{\nu}$

in collaboration with:

Arizona State University, University of British Columbia, Brookhaven National Laboratory, University of Cincinnati, IHEP (Protvino), INR (Moscow), KEK, Kyoto University of Education, Kyoto University, University of Montreal, University of New Mexico, INFN, University of Perugia, Stony Brook University, TRIUMF, Tsinghua University (Beijing), University of Virginia, Virginia Polytechnic Institute and State University, and Yale University.

The scientific motivations, techniques, and instrumentation associated with the KOPIO measurement of the $K_L^0 \rightarrow \pi^0 \nu \bar{\nu}$ branching ratio have been discussed in previous annual reports. Many promising approaches to physics beyond the Standard Model (SM) will be tested by

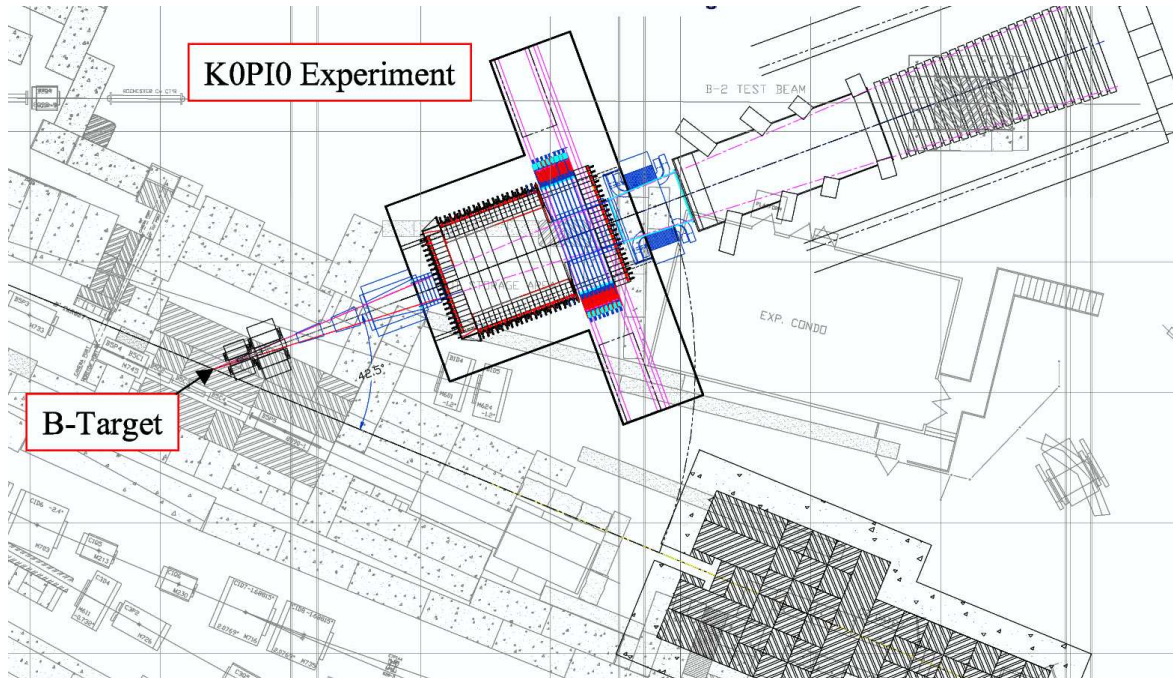


Figure 4.3:

Floor layout of the KOPIO detector. The 25.5 GeV/c proton beam extracted from the AGS hits the KOPIO target before reaching the beam dump shown in the bottom right. The secondary beam line selects neutral particles emitted at 42.5° using collimators and sweeping magnets. The channel has an acceptance of 90 mr horizontally and 4 mr vertically. Photons are strongly suppressed with the help of a *spoiler*, a 5 cm thick lead plate at the entrance of the channel. See last year's report for details on the setup.

this high sensitivity measurement, and the results will be complementary to measurements at the high energy frontier. For instance, if supersymmetry or other new physics were to be discovered at the LHC, the results from KOPIO would be critical for unraveling whether the flavor structure of this new physics is governed by the SM Yukawa couplings (e.g. Minimal Flavor Violation) or whether there are new sources of CP violation with a new flavor structure. In the absence of a non-SM result, KOPIO will obtain a precision of 10% or better on the branching ratio resulting in the single most precise measurement of CP violation. The basic features of the measurement involve a micro-bunched beam of 10^{14} protons on target during each spill of the AGS used to produce an intense carefully collimated neutral kaon beam (see Fig. 4.3). The detection system employing a unique high efficiency, high resolution pointing calorimeter is used to identify the single π^0 signal in the kaon center-of-mass system while highly efficient photon and charged particle vetos ensure that no other particles were present in coincidence. All important principles of the technique have been tested experimentally with prototypes and/or studied with extensive simulations and construction of the various detector systems will start in October 2005.

Experimental sensitivity

The final error in the measured value of the $K_L^0 \rightarrow \pi^0 \nu \bar{\nu}$ branching ratio depends on the distribution of the number of signal events v.s. the signal to background ratio (S/B). Main sources of background are the decays $K_L^0 \rightarrow 2\pi^0$ and $K_L^0 \rightarrow \pi^0 \pi^+ \pi^-$ when the additional particles remain unobserved. In the case of $K_L^0 \rightarrow 2\pi^0$ two components should be distinguished: *even background* results when the observed photons originate from the same π^0 , *odd background* results when this is not the case. Even background is characterized by a mono-energetic π^0 in the kaon c.m.s. system: $E_{\pi^0}^* = \frac{1}{2} m_K c^2$. The transformation is made possible by the measurement of the kaon time of flight between production target and decay vertex. Odd background can be suppressed kinematically by requiring $m_{\gamma\gamma} = m_{\pi^0}$ within resolution. For the other backgrounds this condition is automatically fulfilled. $K_L^0 \rightarrow \pi^0 \pi^+ \pi^-$ is limited to low values of $E_{\pi^0}^*$. Main measure against background are hermetic veto systems. Since both the photon and the charged particle inefficiencies are strongly energy dependent S/B depends on the missing energy. Based on these considerations the separation of signal and background depends primarily on the following three quantities:

- $T_{\pi^0}^* \equiv E_{\pi^0}^* - m_{\pi^0} c^2$, the π^0 kinetic energy in the kaon center-of-mass system,
- E_{miss} , the missing energy in the laboratory system and
- $m_{\gamma\gamma}$, the 2γ invariant mass.

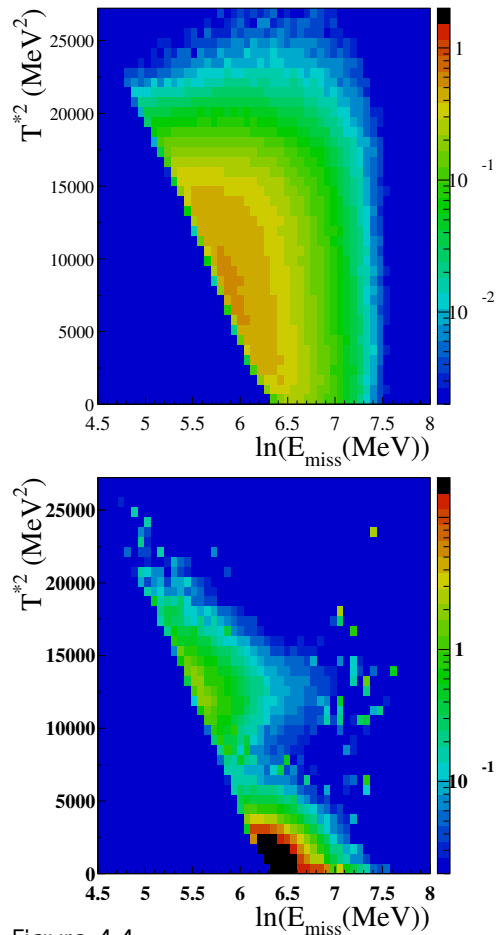


Figure 4.4:
 $T_{\pi^0}^{*2}$ v.s. $\ln E_{\text{miss}}$ for signal (top) and background (bottom) after suppression of events with veto signals. Whereas signal events show a roughly constant distribution over the allowed phase space, backgrounds are concentrated in a low $T_{\pi^0}^{*2}$ region populated by $K_L^0 \rightarrow \pi^0 \pi^+ \pi^-$ decays and a high $T_{\pi^0}^{*2}$ region populated by $K_L^0 \rightarrow 2\pi^0$ even decays.

Figure 4.5:

$K_L^0 \rightarrow \pi^0 \nu \bar{\nu}$ signal for two assumptions for the branching ratio (SM prediction and B vanishing). Events are ordered according to their probability to be signal rather than background. Assuming the central value for the SM prediction the experiment would result in ≈ 50 gold-plated events with S/B around 5. A sample with roughly equal numbers of signal and background events would have $S \approx B \approx 200$.

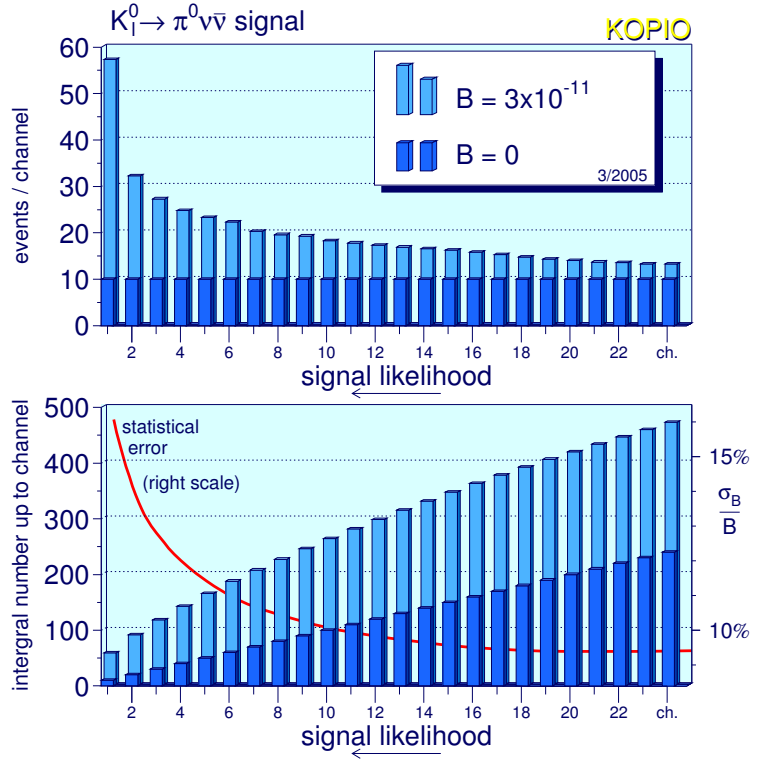


Figure 4.4 shows simulated distributions of $T_{\pi^0}^{*2}$ vs. $\ln E_{\text{miss}}$ for both signal and total background after suppression of events with signals in the veto systems. From these distributions the probability of an event to be either signal or background can be calculated. The resulting distributions are shown in Fig. 4.5. From these distributions a statistical uncertainty below 10% can be estimated which corresponds to a precision of 5% for the area of the unitarity triangle.

Charged-particle veto system

The purpose of the Charged Particle Veto (CPV) is to provide an efficient identification of background processes in which an apparent $\pi^0 \rightarrow 2\gamma$ decay inside the decay volume is accompanied by charged particle emission. Examples of such background processes are $K_L^0 \rightarrow \pi^+ \pi^- \pi^0$, $K_L^0 \rightarrow \pi^0 \pi^\pm e^\mp \nu$, $K_L^0 \rightarrow \pi^\pm e^\mp \nu \gamma$ in which the e^\mp creates a second photon through Bremsstrahlung or e^\pm annihilation in flight, and $K_L^0 \rightarrow e^+ \pi^- \nu$, again followed by $e^+ \rightarrow \gamma$ whereas the π^- creates a photon through $\pi^- p \rightarrow \pi^0 n$. In all cases, two particles with opposite electrical charge emerge. Charged-particle detection efficiencies of 99.99% or better are required to keep these backgrounds below 10% in most kinematic regions.

The design of the CPV is based on requirements resulting from extensive simulations of the various background processes and our own tests of the momentum dependence of the detector response to various charged particles (π^\pm, μ^\pm, e^\pm). The intrinsic charged particle detection efficiency should be $> 99.99\%$. Inefficiencies are caused by (π^-, xn) reactions, backscattering, or positron annihilation in flight. Our tests show that the efficiency requirement is met if the dead layer in front of the CPV is kept below 20 mg/cm^2 and the detection threshold is kept below 50 keV. The first requirement can only be met when the detectors are situated inside the decay tank and/or beam pipe. With the possible exception of the up-

stream beam hole, the detector has to extend to the full 4π sr. This requires in particular that particles moving downstream within the beam envelope have to be observed as well. In order to separate π^0 decays from (n,π^0) reactions in the CPV from the events of interest the detector elements have to be kept more than 50 cm from the fiducial decay volume. The spread in the time difference between the decay time as reconstructed from the $\pi^0 \rightarrow 2\gamma$ decay kinematics and the signals observed in the CPV should be within 12 ns to avoid accidental vetoing by CPV signals from neighboring beam bunches. This requirement sets limits to the intrinsic time resolution and the granularity of the CPV. Depending on the algorithm used to analyze the digitized wave forms, veto signals may get lost when preceded by another signal in the same detector element. These losses are minimized by using fast detectors which are as thin as possible and by distributing the load over many channels. Since access will be limited to less than a few times per year, the loss of a few readout channels must not result in substantial data loss. This requirement can be met by redundancy in the readout of each individual detector element.

The Charged Particle Veto consists of three plastic scintillator systems. Our group is responsible for the Barrel CPV (see Fig. 4.6)

which consists of 2-mm-thick tiles of Bicron BC408 plastic scintillator covering the walls of the decay tank with the exception of the regions where the beam crosses. The Downstream CPV lines the downstream beam pipe where it crosses the photon detectors. This system is followed by a sweeping magnet and associated veto counters.

Time schedule

The KOPIO construction phase will last about five years starting in October 2005. It is our intention to finish production of the barrel CPV early in the year 2007. Installation at BNL would take place towards the end of 2008.

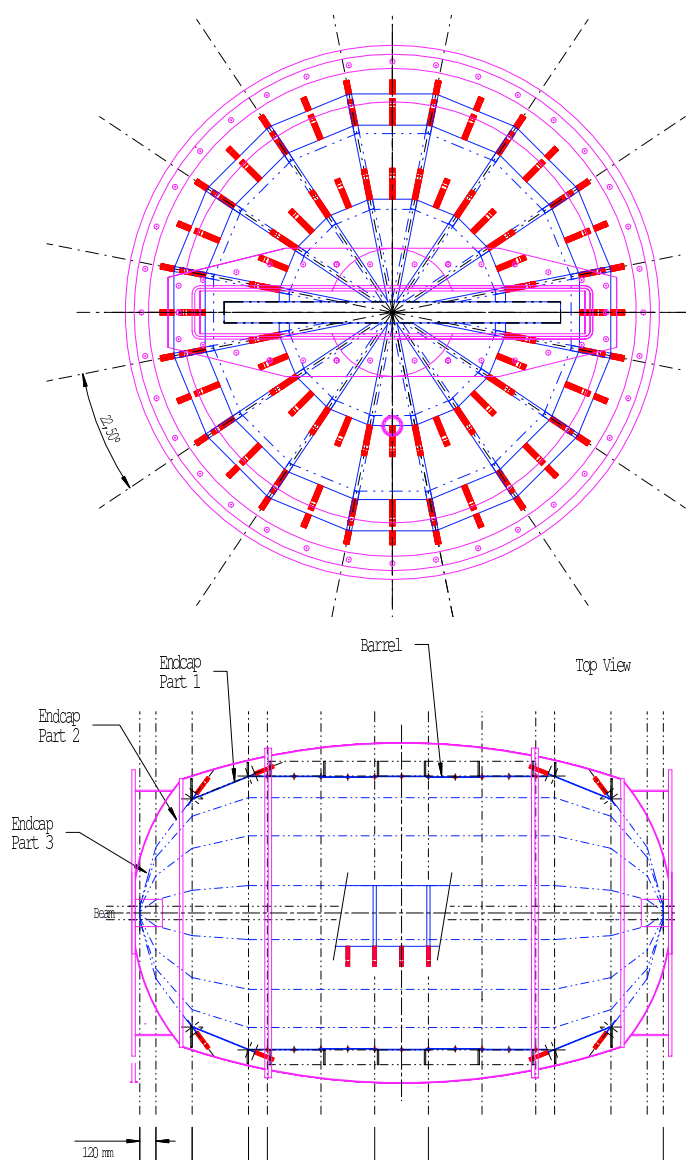


Figure 4.6:
End-cap view (top) and horizontal cross section (bottom) of the barrel CPV.